

# Enhancing Targeted Attack Transferability via Diversified Weight Pruning

Hung-Jui Wang, Yu-Yu Wu, Shang-Tse Chen

National Taiwan University, Taiwan  
 {r10922061, r10922018, stchen}@csie.ntu.edu.tw

## Abstract

Malicious attackers can generate targeted adversarial examples by imposing human-imperceptible noise on images, forcing neural network models to produce specific incorrect outputs. With cross-model transferable adversarial examples, the vulnerability of neural networks remains even if the model information is kept secret from the attacker. Recent studies have shown the effectiveness of ensemble-based methods in generating transferable adversarial examples. However, existing methods fall short under the more challenging scenario of creating targeted attacks transferable among distinct models. In this work, we propose Diversified Weight Pruning (DWP) to further enhance the ensemble-based methods by leveraging the weight pruning method commonly used in model compression. Specifically, we obtain multiple diverse models by a random weight pruning method. These models preserve similar accuracies and can serve as additional models for ensemble-based methods, yielding stronger transferable targeted attacks. Experiments on ImageNet-Compatible Dataset under the more challenging scenarios are provided: transferring to distinct architectures and to adversarially trained models. The results show that our proposed DWP improves the targeted attack success rates with up to 4.1% and 8.0% on the combination of state-of-the-art methods, respectively.

## 1 Introduction

While deep learning continues to achieve breakthroughs in various domains, recent studies have shown vulnerabilities of deep neural networks to adversarial attacks, causing severe threats in safety-critical applications. For example, in image classification, an attacker can create adversarial examples by adding human-imperceptible perturbations to benign images at test. These adversarial images can mislead a well-trained convolution neural network (CNN) to yield arbitrary classification results. Several adversarial attacks have been proposed to improve and evaluate (Carlini and Wagner 2017; Tramèr et al. 2018; Li et al. 2019) the robustness of CNNs.

In the white-box settings, with full information of the victim model, adversarial examples can be generated effectively and efficiently. In the black-box settings, where the attacker only has limited information of the victim model, it is still possible to create cross-model attacks by using a substitute model with white-box adversarial attack methods.

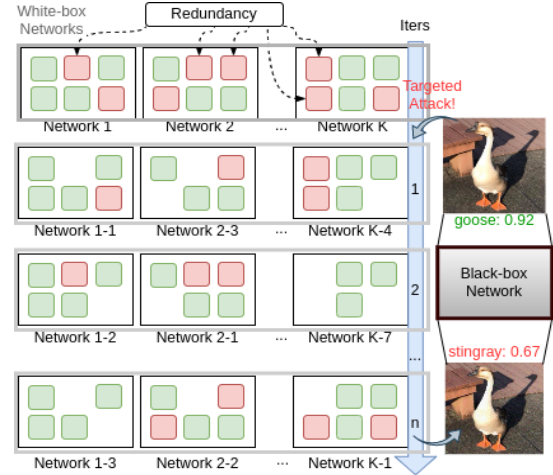


Figure 1: **The big picture of DWP.** Based on the over-parameterized property of neural networks, we leverage weight pruning to produce additional diversified newborn models from existing white-box networks at each iteration. Since weight pruning only removes redundancy in each network, the quality of models is well-preserved. These additional diversified models benefit current ensemble-based approaches for transferable targeted attacks.

This kind of black-box attacks depend on the property of transferability among different CNN models.

Many methods have been proposed to increase the transferability for untargeted attacks, where the goal is to decrease the accuracy of the victim model. However, there is still room for improvement in creating transferable targeted attacks, where the attacker need to mislead the victim model to produce a predefined specific outcome.

Recent work use an ensemble-based approach to generate transferable targeted adversarial examples with multiple CNNs models (Liu et al. 2017; Zhao, Liu, and Larson 2021).

Inspired by the benefit of utilizing multiple CNNs simultaneously, we further enhance the ensemble-based approach by creating more CNN models from a small set of white-box models. We focus on generating transferable targeted adversarial examples on the classical image classification task, proposing a novel approach named Diversified Weight Pruning (DWP). Weight pruning (Han et al. 2015) is a tech-

nique commonly used in model compression. Prior work has shown that neural networks are often over-parameterized (Denil et al. 2013), and proposed methods to remove redundancy (LeCun, Denker, and Solla 1989; Han et al. 2015; Frankle and Carbin 2019; Liu et al. 2019).

We apply random weight pruning to each single CNN network accessible to form additional ones. These additional pruned networks with certain diversity can still preserve high accuracies comparable to that of the original model. We thus improve the ensemble-based approach with these extra diverse models.

To evaluate DWP, we experiment with an ImageNet-compatible dataset used in the NIPS 2017 adversarial competition (Kurakin et al. 2018). The average targeted success rate of our proposed DWP reaches 95.22% on the commonly adopted networks. Furthermore, we follow (Zhao, Liu, and Larson 2021) and test DWP in the more challenging scenarios of transferring to adversarially trained models and to distinct architectures. The results show that DWP can improve the targeted success rate with up to 8.0% and 4.1% on average in these two setting, respectively.

In summary, our primary contributions are as follows:

- We propose a novel approach DWP leveraging weight pruning to enhance the ensemble-based method for transferable targeted attacks, which is compatible with most of the current techniques.
- Our proposed DWP is lightweight and portable without extra data or network training.
- The experiment results show that DWP remains effective in the more challenging settings of transferring to adversarially trained models or to distinct model architectures
- We analyze cosine similarity between perturbations acquired by attacking different pruned networks. It supports the claim that weight pruning increases the diversity of networks for generating adversarial perturbations.

## 2 Related Work

### 2.1 Transferable Attack

In this paper, we focus on simple transferable attacks (Zhao, Liu, and Larson 2021), which require neither additional data nor model training for attacking compared to resource-intensive attacks. Recent works aiming for simple transferable attacks mainly include four categories: gradient calibration, input transformation, advanced loss function, ensemble, and network augmentation.

**Gradient Calibration.** Optimization-based methods are widely adopted (Szegedy et al. 2014; Goodfellow, Shlens, and Szegedy 2015; Carlini and Wagner 2017; Kurakin, Goodfellow, and Bengio 2017) in generating adversarial examples. With iterative methods (Kurakin, Goodfellow, and Bengio 2017; Carlini and Wagner 2017), one can get better solutions to an objective function for attacking through multiple times of optimization on adversarial examples and get stronger attacking results. Adjusting gradients used to update adversarial examples at each iteration appropriately has been shown beneficial for overcoming sub-optimal results in

optimization. (Dong et al. 2018) combines momentum techniques with iterative attacks, accumulating gradients at each iteration to escape local optimum and stable the direction of updating. (Lin et al. 2020) applies Nesterov accelerated gradient for optimization, giving adversarial examples an anticipatory updating to yield faster convergence.

**Input Transformation.** Motivated by Data Augmentation (Shorten and Khoshgoftaar 2019), several works suggest attacking transformed input to prevent adversarial examples from overfitting white-box models and failing to transfer to black-box ones. (Xie et al. 2019) uses random resizing and padding throughout the iterative attack. (Dong et al. 2019) enumerates several translated versions for each input image and fuses the gradients acquired on all of them. (Lin et al. 2020) leverages the scale-invariant property of CNNs and employs multiple scale copies from each input image. (Wang et al. 2021) extends the concept of mixup (Zhang et al. 2018), attacking the mixup version of each input image.

**Modern Loss Function.** Cross entropy loss is widely used in image classification, also serving as the objective function for adversarial attacks. However, for targeted attacks, cross entropy is pointed out the saturation problem (Li et al. 2020a) as the output confidence of target class approaches to one. To this end, alternative loss functions attempt to provide more suitable gradients for optimization. (Li et al. 2020a) leverages Poincaré distance as the loss function, which amplifies the gradient magnitude as the confidence of the target class grows. (Zhao, Liu, and Larson 2021) proposes a simple logit loss, which has constant gradient magnitude regardless of the output probability.

**Ensemble and Network Augmentation.** Adversarial examples generated by ensembling multiple white-box networks are more likely to transfer to black-box networks (Liu et al. 2017). Instead of simply fusing the output confidence of each white-box network, (Xiong et al. 2022) suggests reducing the gradient variance of white-box models during attacking. To further improve ensemble-based approaches, Network Augmentation produces additional diverse models from the existing white-box networks. (Yuan et al. 2021) uses reinforcement learning to automatically find transformations suitable with white-box networks to yield more diversity. (Li et al. 2020b) acquires ghost networks for ensemble through perturbing dropout and skip connections of existing ones. (Duan et al. 2022) further improves the diversified ensemble via dual-stage erosion.

### 2.2 Network Pruning

The intensive cost of computation and storage hinders applications of neural networks, especially on embedding systems. Network Compression aims to reduce the scale of networks, making them more feasible for deployment. With the over-parameterized property (Denil et al. 2013), several works about removing redundancy in networks, known as Network Pruning, are proposed and become a branch of Network Compression. (LeCun, Denker, and Solla 1989) uses the second-derivative information to find redundant weights

in networks. (Han et al. 2015) shows that neural networks can highly preserve performance even if trimming more than half of their connections. Retraining after pruning for better preservation of accuracy is also investigated (Frankle and Carbin 2019; Liu et al. 2019).

### 3 Methodology

To generate a targeted adversarial example  $x^{\text{adv}}$  with target class  $y^{\text{target}}$  for a network  $\theta$  from an benign image with its label  $(x, y)$ , we aim to solve the following constrained optimization problem:

$$\arg \min_{x^{\text{adv}}} J(x^{\text{adv}}, y^{\text{target}}; \theta) \quad \text{s.t.} \quad \|x^{\text{adv}} - x\|_{\infty} \leq \epsilon,$$

where  $J$  is the loss function for multiclass classification, and  $\epsilon$  is the perturbation budget ensuring each adversarial example keeps human-imperceptible. To circumvent the gradient decreasing problem of cross-entropy, we adopt logit loss (Zhao, Liu, and Larson 2021) as our loss function  $J$ .

#### 3.1 Preliminary & Motivation

We start by establishing the roles of current state-of-the-art techniques in our iterative attack. After that, we demonstrate how we apply Weight Pruning to improve targeted transferability.

**Momentum and Nesterov Iterative Method (NI) (Dong et al. 2018; Lin et al. 2020)** Considering that the optimization of the popular Iterative-FGSM method (Kurakin, Goodfellow, and Bengio 2017) may fall into local optimum, Momentum Iterative-FGSM integrates the momentum technique to accumulate historical gradients and stable the update direction. Starting from  $x_1 = x$  and  $g_0 = 0$ , we have the iterative procedure:

$$g_n = \mu \cdot g_{n-1} + \frac{\nabla_x J(x_n, y^{\text{target}}; \theta)}{\|\nabla_x J(x_n, y^{\text{target}}; \theta)\|_1}$$

$$x_{n+1} = \text{Clip}_x^\epsilon(x_n - \alpha \cdot \text{sign}(g_n)).$$

Here  $\mu$  is the decay factor of the historical gradients. The gradient computed encourages adversarial examples to increase confidence logit output by the white-box network model  $\theta$  on the target class through gradient ascent with learning rate  $\alpha$ . A clipping operation onto the  $\epsilon$ -ball centered at the original input image  $x$  is at the end of each iteration.

Inspired by Nesterov Accelerated Gradient (NESTEROV 1983), Nesterov Iterative Method (NI) adds the historical gradients to current adversarial examples  $x_n$  and gets  $x_n^{\text{nes}}$  in advance. Gradients at the ahead  $x_n^{\text{nes}}$  instead of the current  $x_n$  will be used for updating. The scheme helps accelerate convergence by avoiding the local optimum earlier:

$$x_n^{\text{nes}} = x_n + \alpha \cdot \mu \cdot g_{n-1}$$

$$g_n = \mu \cdot g_{n-1} + \nabla_x J(x_n^{\text{nes}}, y^{\text{target}}; \theta)$$

To preserve more information about the gradient for attacking (Zou et al. 2022), we don't include the L1 normalization.

**Scale Invariant Method (SI) (Lin et al. 2020)** Neural networks can preserve output even though the input image  $x$  goes through scale operations such as  $S_m(x) = x/2^m$ . With the scale-invariant property, each composite of white-box networks and scale operations can serve as an augmentation of models. Adversarial examples can enjoy more diversity with these augmented networks:

$$g_n = \mu \cdot g_{n-1} + \frac{1}{M} \sum_{m=0}^{M-1} \nabla_x J(S_m(x_n^{\text{nes}}), y^{\text{target}}; \theta).$$

$M$  is the number of scaled versions feeding into the network for each image.

**Diverse Input Patterns (DI) (Xie et al. 2019)** Inspired by data augmentation techniques (Shorten and Khoshgof-taar 2019) used in network training, DI imposes random re-sizing and padding on each image before it feeds into network models to avoid overfitting. Straightforward cooperation with NI and SI is as follows:

$$g_n = \mu \cdot g_{n-1} + \frac{1}{M} \sum_{m=0}^{M-1} \nabla_x J(S_m(T(x_n^{\text{nes}}, p_{\text{DI}})), y^{\text{target}}; \theta).$$

The introduced  $T$  decides whether to apply DI at each iteration with probability  $p_{\text{DI}}$ , which will degenerate with  $p_{\text{DI}} = 0$ .

**Translation Invariant Method (TI) (Dong et al. 2019)** To deal with different discriminative regions (Dong et al. 2019) of various defense neural networks, TI produces several translated versions for the current image in advance and computes the gradient for each separately. These gradients will then be fused and used to attack the current image. (Dong et al. 2019) also shows that one can approximate the gradient fusion using convolution. The approximation prevents TI from enduring the costly computation on excessive translated versions for every single image, also yielding the further revised updating procedure:

$$g_n = \mu \cdot g_{n-1} + \mathbf{W} * \frac{1}{M} \sum_{m=0}^{M-1} \nabla_x J(S_m(T(x_n^{\text{nes}}, p_{\text{DI}})), y^{\text{target}}; \theta).$$

$\mathbf{W}$  is the convolution kernel matrix applied. Some typical options are linear, uniform, or Gaussian kernel.

**Ensemble-Based Approach (Liu et al. 2017)** (Liu et al. 2017) suggests that if an adversarial example takes effect on multiple accessible white-box networks, it gets more chance to transfer to other black-box models. With the hypothesis, the ensemble-based approach is enrolled and enriches the procedure with multiple white-box models  $(\theta_1, \theta_2, \dots, \theta_K)$  utilized:

$$g_n = \mu \cdot g_{n-1} + \mathbf{W} * \frac{1}{M} \sum_{m=0}^{M-1} \sum_{k=1}^K \beta_k \nabla_x J(S_m(T(x_n^{\text{nes}}, p_{\text{DI}})), y^{\text{target}}; \theta_k),$$

where  $\beta_k$  are the ensemble weights,  $\sum_{k=1}^K \beta_k = 1$ . We abbreviate the attacking procedure so far to NI-SI-TI-DI-FGSM with the combination of these techniques.

Motivated by the current methods emphasizing diversity for generating adversarial examples, we aim to acquire more diversified white-box networks from the given ones  $\theta_1, \theta_2, \dots, \theta_k$  to boost the ensemble-based approach. Research about Network Compression has shown that Weight Pruning can preserve accuracy even with removing up to 50% of connections in the original network (Han et al. 2015). In other words, each  $\theta_k$  can produce numerous newborn networks  $\theta_{k1}, \theta_{k2}, \dots, \theta_{kL}$  with comparable accuracy to itself through selecting  $L$  different groups of its minor connections and pruning them away. We extend the ensemble-based approach in the above updating procedure:

$$g_n = \mu \cdot g_{n-1} + \frac{W}{M} * \sum_{m=0}^{M-1} \sum_{k=1}^K \sum_{l=1}^L \beta_{kl} \nabla_x J(S_m(T(x_n^{\text{nes}}, p_{\text{DI}})), y^{\text{target}}; \theta_{kl}),$$

where  $\beta_{kl}$  are the ensemble weights,  $\sum_{k=1}^K \sum_{l=1}^L \beta_{kl} = 1$ .

### 3.2 Diversified Weight Pruning

Instead of producing all the newborn models beforehand, we integrate our weight pruning method into the iterative attacking. We acquire newborn models at each iteration right before gradient computing. Without keeping all of them simultaneously, storage and memory overhead are almost identical to the original ensemble-based approach.

We name the proposed approach Diversified Weight Pruning (DWP) due to the increased diversity of white-box models for ensemble via Weight Pruning.

To guarantee the newborn model has acceptable performance as the original one, we sort the connections of each white-box network by the L1 norm of their weight values. With a predefined rate  $r$ , we only consider the lowest  $(100 \cdot r)\%$  “prunable” since weights with small values are shown unnecessary (Han et al. 2015). Networks can preserve accuracy after these connections are pruned away even without retraining (Han et al. 2015).

For our pruning operation, we first identify the set of prunable weights. Let  $\gamma$  be the  $(100 \cdot (1 - r))$ -th percentile of weights in  $\theta$ . We formulate the prunable set:

$$\Gamma(\theta, r) = \{w \in \theta | w < \gamma\} \subseteq \theta.$$

With  $\Gamma(\theta, r)$  collecting all the prunable weights of  $\theta$ , we introduce an indicator vector for it:

$$\Pi_{\Gamma(\theta, r)} = (\lambda_1, \lambda_2, \dots, \lambda_\kappa),$$

where  $\kappa$  is the total number of weights in  $\theta = \{w_1, w_2, \dots, w_\kappa\}$  including non-prunable ones.  $\lambda_i$  is determined by whether its corresponding  $w_i \in \theta$  is in the prunable subset  $\Gamma(\theta, r)$ :

$$\lambda_i = \begin{cases} 1, & \text{if } w_i \in \Gamma(\theta, r) \\ 0, & \text{otherwise} \end{cases}.$$

Supported by the indicator vector  $\Pi_{\Gamma(\theta, r)}$ , our pruning operation  $P(\cdot)$  can protect the non-prunable weights by masking:

$$P(\theta, r) = (\mathbf{1}_\kappa - \Pi_{\Gamma(\theta, r)} \odot \mathbf{b}) \odot \theta,$$

where  $\odot$  denotes the element-wise multiplication and  $\mathbf{1}_\kappa = (1, 1, \dots, 1) \in R^\kappa$  denotes an all-one vector.  $\mathbf{b} = (b_1, b_2, \dots, b_\kappa)$  is a vector with  $b_i \stackrel{\text{i.i.d}}{\sim} \text{Bernoulli}(p_{\text{bern}})$ .

To be specific,  $\Pi_{\Gamma(\theta, r)}$  and  $\mathbf{b}$  both are binary masks with identical layout as  $\theta$ .  $\Pi_{\Gamma(\theta, r)}$  is responsible for protecting non-prunable weights, while  $\mathbf{b}$  is for random pruning. Each binary element in  $\Pi_{\Gamma(\theta, r)} \odot \mathbf{b}$  indicates whether to prune the corresponding weight value in  $\theta$ . The main difference from a similar technique, Dropout (Srivastava et al. 2014; Li et al. 2020b), is that DWP only considers prunable weights. We will show the significance of protecting non-prunable weights in Ablation Study. Once we obtain the gradients, we will revoke the pruning operation to keep the white-box networks intact for successive iterations.

With the participation of DWP, we extend the abbreviation as DWP-NI-SI-TI-DI-FGSM, further modifying our updating scheme:

$$g_n = \mu \cdot g_{n-1} + \frac{W}{M} * \sum_{m=0}^{M-1} \sum_{k=1}^K \beta_{kl} \nabla_x J(S_m(T(x_n^{\text{nes}}, p_{\text{DI}})), y^{\text{target}}; P(\theta_k, r)).$$

Since we’re not aiming for actually compressing networks, the pruning operations only mask unwanted connections rather than truly delete them. Thus, the layout of each network is hardly affected, allowing DWP to be more portable and usable. Also, benefiting from no dependency on network retraining and extra data, our proposed DWP is simple and lightweight. As there is no further retraining, we select the L1 norm for pruning since it is better than L2 on preserving accuracy (Han et al. 2015).

## 4 Experiments

### 4.1 Experimental Setup

**Dataset.** To evaluate targeted attack, we use an ImageNet-compatible dataset<sup>1</sup> provided by NIPS 2017 adversarial competition (Kurakin et al. 2018) containing 1,000 images. Each image in the dataset has an officially assigned target class for consistency.

**Networks.** We perform experiments on eight naturally trained models: Inception-v3 (Inc-v3) (Szegedy et al. 2016), Inception-v4 (Inc-v4), Inception-Resnet-v2 (IncResv2) (Szegedy et al. 2017), ResNet-50 (Res-50), ResNet-101 (Res-101), ResNet-152 (Res-152) (He et al. 2016), VGGNet-16 (VGG-16) (Simonyan and Zisserman 2015) and DenseNet-121 (Den-121) (Huang et al. 2017), and two adversarially trained models: ens3-adv-Inception-v3 (Inc-v3ens3) and ens-adv-inception-resnet-v2 (IncRes-v2ens) (Tramèr et al. 2018). All the ten networks are publicly accessible.

**Hyper-parameters.** Our method includes three input transformations TI, DI, and SI. We follow (Li et al. 2020a), setting the probability  $p_{\text{DI}}$  of DI to be 0.7 and selecting a Gaussian kernel with the kernel length equaling 5 for  $W$  in

<sup>1</sup>[https://github.com/cleverhans-lab/cleverhans/blob/11ea10/examples/nips17\\_adversarial\\_competition/dataset/dev\\_dataset.csv](https://github.com/cleverhans-lab/cleverhans/blob/11ea10/examples/nips17_adversarial_competition/dataset/dev_dataset.csv)

TI. For SI, due to the limitation in computing resources, we set the number of scale copies  $M = 3$ . Following (Dong et al. 2018; Lin et al. 2020; Li et al. 2020a; Zhao, Liu, and Larson 2021), the momentum decay factor  $\mu$  is assigned 1. As for the total iteration for iterative attacks, we conduct experiments under 20 and 100 respectively with learning rate  $\alpha = 2/255$  following (Zhao, Liu, and Larson 2021) to observe results under the different extent of converging. All the experiments comply with perturbations less than the budget  $\epsilon = 16$  under  $L_\infty$  norm to keep adversarial examples imperceptible to humans. Last but not least, for our proposed DWP, the probability  $p_{\text{bern}}$  is 0.5 and the prunable rate  $r$  is 0.7, which means at each iteration, we prune 35% of connections of each network in expectation.

**Baseline Methods.** To inspect the compatibility of DWP, we consider the entire NI-SI-TI-DI-FGSM and each of its components as our baselines. We expect DWP to improve each technique alone. The middle column of Table 1 summarizes abbreviations of our baseline methods and their relations to the hyper-parameters, which are NI-FGSM, SI-FGSM, TI-FGSM, DI-FGSM, and NI-SI-TI-DI-FGSM.

Hyper-parameters	NI-SI-TI-DI-FGSM	DWP-NI-SI-TI-DI-FGSM
$M = 0, p_{\text{DI}} = 0$ , Identity kernel $W$ (Gonzalez 2009)	NI-FGSM	DWP-NI-FGSM
$\mu = 0, M = 0, p_{\text{DI}} = 0$	TI-FGSM	DWP-TI-FGSM
$\mu = 0, M = 0$ , Identity kernel $W$	DI-FGSM	DWP-DI-FGSM
$\mu = 0, p_{\text{DI}} = 0$ , Identity kernel $W$	SI-FGSM	DWP-SI-FGSM

Table 1: The abbreviations of baseline methods. For example, TI-FGSM is the special case of NI-SI-TI-DI-FGSM with  $\mu = 0$ ,  $M = 0$  and  $p_{\text{DI}} = 0$ . DI-FGSM, NI-FGSM and SI-FGSM are also special cases under certain hyper-parameters. DWP will be combined with each baseline method for evaluation.

## 4.2 Transferable Targeted Attack in various scenarios

We consider targeted transferability under three scenarios: common transferring, transferring to distinct architectures and transferring to adversarially trained models. We will prepare specified networks for each case. Each time we select a network as the black-box model and take the others as white-box models. We generate adversarial examples on the ensemble of the white-box models and evaluate targeted success rates on the black-box model left alone. No access to the black-box model is allowed during attacking. Note that for ensembling, we use equal ensemble weights  $\beta_k = 1/K$  for each of the  $K$  white-box models.

**Common Transferring** In common transferring, we select Inc-v3, Inc-v4, IncResv2, Res-50, Res-101, and Res-152. The six normally trained networks are commonly adopted to provide a preliminary estimation of the transferability of attacks (Dong et al. 2018; Xie et al. 2019; Dong et al. 2019; Li et al. 2020a; Zhao, Liu, and Larson 2021) for evaluation.

Table 2 shows results of transferable targeted attack under the common transferring scenario. DWP boosts almost all

the attack methods, especially the standalone ones. When all the state-of-the-art techniques collaborate with DWP, the average targeted success rate can even achieve 95.22%.

**Transferring to Distinct Architectures** In general, information about the networks used by defenders remains unknown to attackers. A targeted attack method will be more practical if adversarial examples generated can transfer to black-box architectures less similar to the white-box networks utilized by attackers. Therefore, we follow (Zhao, Liu, and Larson 2021) and evaluate the attack methods on the four networks with distinct architectures: Res-50, VGG-16, Den-121, and Inc-v3.

Results of transferring to distinct architectures are shown in Table 3. Due to the less similarity between networks’ architectures, there is more room for improvement on targeted transferability under the scenario than the common transferring. DWP enhances NI-SI-TI-DI-FGSM with 4.1% on average after 100 iterations, which is more than 1.5% under the common transferring. These results demonstrate the benefits of diversified ensemble in attacking distinct black-box architectures.

**Transferring to Adversarially Trained Models** Adversarial training (Tramèr et al. 2018; Madry et al. 2018) is one of the primary techniques for defending against malicious attacking. It brings robustness to models by training them with adversarial examples. Under the scenario of transferring to adversarially trained models, we ensemble only the six naturally trained networks (Inc-v3, Inc-v4, Inc-cResv2, Res-50, Res-101, and Res-152) as white-box models to simulate the situation where attackers have few details about defense. The two adversarially trained networks (Inc-v3ens3 and IncRes-v2ens) will act as our black-box model separately.

Table 4 summarizes the results of transferring to adversarially trained networks. Targeted success rates under this scenario are lower than the other two due to the robustness of adversarially trained networks. Under such a challenging scenario, DWP still helps alleviate the discrepancy between white-box naturally trained and black-box adversarially trained networks, bringing about up to 8.0% and 6.75% improvement on average under 20 and 100 iterations. The necessity of the diversified ensemble is highlighted again, especially for black-box networks with significant differences from white-box ones.

## 4.3 Perturbations from Different Newborn Models

(Liu et al. 2017) observes that adversarial perturbations from white-box neural networks with different architectures will be orthogonal. The orthogonality implies zero cosine similarity, implying diversity to a certain degree. Since DWP produces additional newborn models, the relationship between perturbations generated from these models is noteworthy. In this section, we analyze perturbation vectors from newborn models belonging to identical networks and different networks using cosine similarity following (Liu et al. 2017).

Attack Method	-Inc-v3	-Inc-v4	-IncRes-v2	-Res-50	-Res-101	-Res-152	Average
TI-FGSM	21.5/24.2	21.1/25.1	23.8/29.1	52.2/63.6	56.4/71.4	53.9/67.5	38.15/46.82
DWP-TI-FGSM	24.1/43.9	24.8/46.6	25.3/53.1	55.6/78.7	63.0/84.0	57.8/83.0	<b>41.77/64.88</b>
DI-FGSM	55.7/78.4	57.7/81.8	59.0/84.4	67.7/91.2	71.1/91.9	73.0/93.4	64.03/86.85
DWP-DI-FGSM	59.8/87.4	60.7/89.5	62.3/89.1	70.1/93.7	73.5/93.9	74.4/94.7	<b>66.80/91.38</b>
NI-FGSM	18.8/35.9	16.7/35.1	17.8/36.9	45.3/63.1	50.0/66.7	49.2/67.9	32.97/50.93
DWP-NI-FGSM	31.7/50.9	26.3/49.1	28.6/53.4	58.7/74.6	64.7/80.3	61.6/81.3	<b>45.27/64.93</b>
SI-FGSM	39.5/41.5	35.8/38.4	38.0/43.1	66.5/75.7	71.2/79.8	71.0/79.5	53.67/59.67
DWP-SI-FGSM	40.9/64.7	42.0/66.4	47.1/72.0	72.6/89.7	76.8/91.6	77.5/91.9	<b>59.48/79.38</b>
NI-SI-TI-DI-FGSM	71.1/91.3	75.1/92.7	76.3/92.7	81.7/94.4	84.0/95.5	85.5/95.6	78.95/93.70
DWP-NI-SI-TI-DI-FGSM	<b>77.2/94.1</b>	<b>79.3/94.1</b>	<b>78.9/94.3</b>	<b>82.3/95.8</b>	<b>85.1/96.3</b>	<b>87.2/96.7</b>	<b>81.67/95.22</b>

Table 2: The targeted success rates (%) of common transferring. “-” in each column stands for the black-box network while the other five serve as white-box ones for ensemble. Each cell is of results under 20/100 iterations. DWP improves all the methods, especially for the standalone ones.

Attack Method	-Res-50	-Den-121	-VGG16	-Inc-v3	Average
TI-FGSM	17.7/25.2	20.3/28.1	22.3/30.3	6.3/8.8	16.65/23.10
DWP-TI-FGSM	21.3/42.0	25.5/41.5	27.5/55.4	7.7/15.7	<b>20.50/38.65</b>
DI-FGSM	39.1/67.3	44.8/76.3	47.9/75.5	24.7/49.5	39.13/67.15
DWP-DI-FGSM	40.9/73.0	49.0/80.1	51.3/82.6	25.1/54.8	<b>41.58/72.63</b>
NI-FGSM	13.2/27.1	17.0/33.4	15.9/30.6	6.8/17.4	13.23/27.13
DWP-NI-FGSM	19.3/36.2	22.6/43.9	28.4/46.6	8.9/20.5	<b>19.80/36.80</b>
SI-FGSM	28.2/34.5	35.1/45.5	29.1/38.0	13.6/16.8	26.50/33.70
DWP-SI-FGSM	33.4/54.1	40.4/61.7	42.7/64.7	16.2/27.4	<b>33.18/51.98</b>
NI-SI-TI-DI-FGSM	57.6/80.6	70.3/88.1	60.4/80.2	48.1/72.0	59.10/80.23
DWP-NI-SI-TI-DI-FGSM	<b>59.7/83.1</b>	<b>72.9/90.4</b>	<b>63.8/86.8</b>	<b>49.5/77.0</b>	<b>61.48/84.33</b>

Table 3: The targeted success rates of transferring to distinct architectures. “-” stands for the black-box network with the other three serving as the white-box ones for ensemble. Each cell is of results under 20/100 iterations. DWP appears to be compatible with each of these state-of-the-art techniques, yielding improvement with them on average.

We study the four networks same as transferring to distinct architectures. Firstly, we acquire five newborn models from each of the four networks via pruning different connections. For calculating cosine similarity between perturbations, we take the average of the first ten images from the ImageNet-compatible dataset to avoid cherry-picking. To prevent the influence of factors other than newborn models, we use NI-FGSM only to generate adversarial perturbations excluding TI, DI, and SI. Note that all the other hyperparameters are the same as attacking. Unlike DWP, we don’t revoke pruning in this experiment to ensure each perturbation is from an identical newborn model throughout attacking.

For perturbations from newborn models belonging to the same architecture, we take ResNet-50 as an example, summarizing the cosine similarity in Table 5. The five newborn models of ResNet-50 yield ten ( $C_5^5$ ) non-diagonal values in pair and five diagonal values with themselves. The diagonal ones are all 1.0 since they are from two identical perturbation vectors. As for the non-diagonal, all the values are close to 0, implying orthogonality. The results show that even

though these newborn models are from the same architecture (ResNet-50) with merely different connections pruned, perturbations generated with them will still be orthogonal as observed in different architectures (Liu et al. 2017).

For perturbations from newborn models belonging to two different architectures and also the cases of single architectures besides ResNet-50, we summarize the average cosine similarity in Table 6. Each diagonal cell ( $i, i$ ) averages cosine similarity from the 10 pairs ( $C_2^5$ ) of five newborn models of the architecture  $i$  (column). The non-diagonal cells ( $i, j$ ) averages the one from 25 pairs of newborn models of architecture  $i$  (row) and  $j$  (column) respectively. All the values in Table 6 are close to zero, suggesting that whether two newborn models belong to the same or different architectures, perturbations generated from them will always be nearly orthogonal.

From the viewpoint of geometry, orthogonal perturbations from various networks participating in the ensemble-based approach enrich the overall direction for updating adversarial examples. These observations on orthogonality support our claim that newborn models obtained via Weight Pruning

Attack Method	Inc-v3ens3	IncRes-v2ens	Average
TI-FGSM	6.0/3.7	1.1/0.2	3.55/1.95
DWP-TI-FGSM	6.8/10.3	1.5/0.7	<b>4.15/5.5</b>
DI-FGSM	23.0/27.5	3.6/2.0	13.3/14.75
DWP-DI-FGSM	25.3/42.1	5.3/4.9	<b>15.3/23.50</b>
NI-FGSM	3.7/9.9	0.3/0.6	2.00/5.25
DWP-NI-FGSM	8.1/11.9	1.0/1.1	<b>4.55/6.50</b>
SI-FGSM	17.2/15.3	4.1/1.0	10.65/8.15
DWP-SI-FGSM	17.7/30.4	5.0/3.8	<b>11.35/17.10</b>
NI-SI-TI-DI-FGSM	55.2/77.7	43.6/54.8	49.40/66.25
DWP-NI-SI-TI-DI-FGSM	<b>64.1/83.1</b>	<b>50.7/62.7</b>	<b>57.40/72.90</b>

Table 4: The targeted success rates of transferring to adversarially trained networks. Adversarial examples are generated by ensembling only the six naturally trained networks in Table 2. Each cell is of success rates under 20/100 iterations. The results show that DWP can alleviate the differences between naturally and adversarially trained networks, improving attacks under the challenging scenario.

Res-50	newborn1	newborn2	newborn3	newborn4	newborn5
newborn1	1.0000	0.0009	0.0005	0.0000	-0.0004
newborn2	-	1.0000	0.0006	-0.0010	-0.0004
newborn3	-	-	1.0000	0.0002	0.0005
newborn4	-	-	-	1.0000	0.0002
newborn5	-	-	-	-	1.0000

Table 5: The perturbation cosine similarity between newborn models belonging to Res-50. Although the models are all acquired from Res-50, their perturbations are still orthogonal. Note that the table is symmetric with the values rounded to four decimal places.

provide more diversity for attacking.

#### 4.4 Ablation Study

In this section, we conduct ablation experiments to study the two key points of DWP: the quality and the quantity of pruning.

**Quality of Pruning: In Comparison with Dropout.** While Weight Pruning considers the importance of each connection and only prunes the redundant ones away, Dropout (Srivastava et al. 2014; Li et al. 2020b) deactivates activation functions without any examination of their values. The reason is that instead of compressing networks, Dropout is mainly used to prevent networks from overfitting (Srivastava et al. 2014) during training. In this section, we produce newborn models using Dropout, comparing the results of targeted attacks with DWP. In the following experiments, we will show considering connection values to guarantee the quality of newborn models is necessary.

Dropout can be viewed as a special case of our Diversified Weight Pruning with all the connections in a network treated as prunable regardless of their weight values. Therefore, we simulate Dropout with the prunable rate  $r$  set to 1.0, giving DWP-NI-SI-TI-DI-FGSM with  $r = 1.0$  an alias, Dropout-NI-SI-TI-DI-FGSM. Both DWP-NI-SI-TI-DI-FGSM with our original settings ( $r = 0.7$ ) and the newly introduced Dropout-NI-SI-TI-DI-FGSM will serve for generating adversarial examples under the scenario of transferring to distinct architectures. We evaluate their targeted success rates

	Res-50	VGG-16	Den-121	Inc-v3
Res-50	0.0001	-0.0001	0.0003	-0.0001
VGG-16	-	0.0004	0.0000	-0.0002
Den-121	-	-	-0.0001	0.0001
Inc-v3	-	-	-	0.0005

Table 6: The average perturbation cosine similarity between each pair of architectures. The non-diagonal cells take an average on 25 pairs of newborn models from the two corresponding architectures, while the diagonal ones average ten. The table shows newborn models of whether distinct or identical architectures yield orthogonal perturbations.

on the black-box model every five iterations for more precise observation.

Results of the comparison between DWP-NI-SI-TI-DI-FGSM and Dropout-NI-SI-TI-DI-FGSM are shown in Figure 2. NI-SI-TI-DI-FGSM is also included for reference. Roughly, targeted attack success rates of all the methods on the four black-box networks increase with more iterations (Zhao, Liu, and Larson 2021). With a closer look, DWP-NI-SI-TI-DI-FGSM in orange curves is much better than all the other methods. The green curves standing for Dropout-NI-SI-TI-DI-FGSM are found even worse than the blue ones of our baseline NI-SI-TI-DI-FGSM. The relatively poor results of Dropout-NI-SI-TI-DI-FGSM are due to the ignorance of weight values when pruning, which may yield newborn models with unstable performance and mislead the directions of targeted adversarial perturbations.

**Quantity of Pruning: Influence of Prunable Rates.** In this section, we focus on targeted attack success rates under different prunable rates. As the prunable rate determines the number of connections possible to be pruned during attacking, white-box models can produce more diverse newborn models using higher prunable rates. However, with an excessive number of connections pruned away, the quality of newborn networks will be unstable.

To find the sweet spot to the trade-off, we enumerate different prunable rates, conducting the attack experiments with all the other hyper-parameters as default. We consider the four models of transferring to distinct architectures since the scenario is closer to the real situation. Moreover, we will provide observations on accuracy decay regarding pruning for reference using the 1,000 clean images of the ImageNet-compatible dataset.

As shown in Figure 3a, the curves of targeted attack success rates excluding each black-box network are roughly mountain-like due to the trade-off. We select  $r = 0.7$  throughout our experiments as the curves reach maximum success rates with the prunable rate. Figure 3b shows the accuracy decay in respect of the ratio of connections pruned in each network. With our designated prunable rate  $r = 0.7$ , DWP will prune 35% of connections approximately. According to Figure 3b, there is no apparent damage to the accuracy of each network with the quantity of pruning. Therefore, the quality of newborn models remains stable.



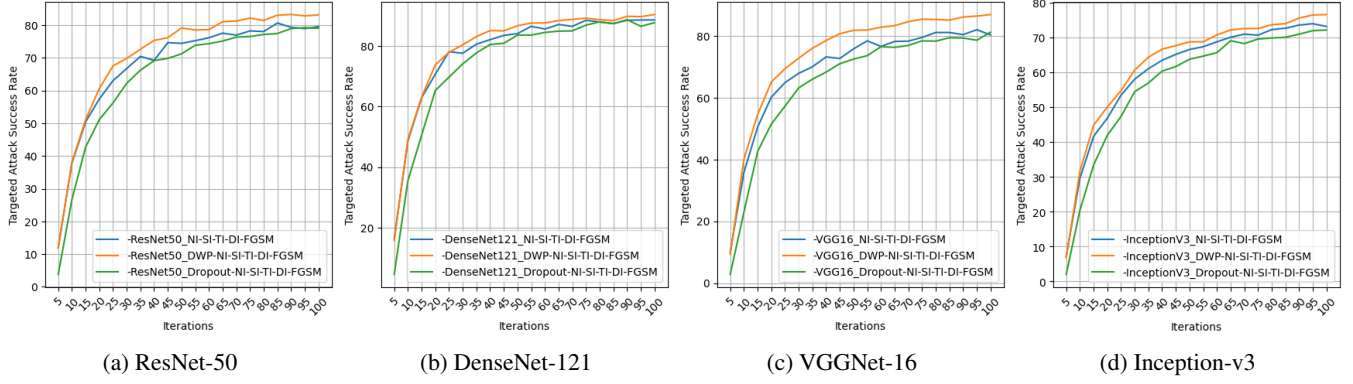


Figure 2: **Comparison between DWP-NI-SI-TI-DI-FGSM, Dropout-NI-SI-TI-DI-FGSM, and our baseline NI-SI-TI-DI-FGSM on targeted transferability with different numbers of iterations.** Each curve shows targeted success rates on the black-box network specified in the caption below. Our DWP-NI-SI-TI-DI-FGSM (orange) is much better than the baseline (blue) and Dropout-NI-SI-TI-DI-FGSM (green). The results demonstrate the significance of protecting necessary weights and ensuring the quality of newborn models for ensembling.

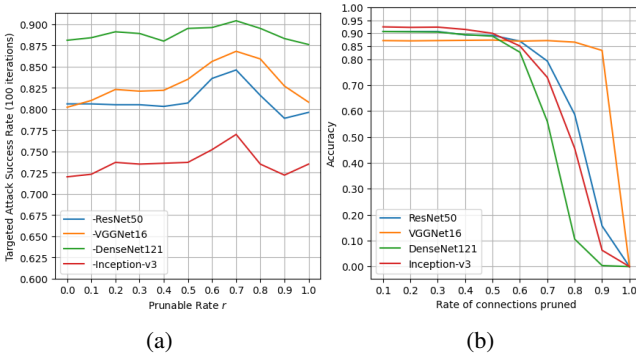


Figure 3: (a): **The targeted success rates under different prunable rates  $r$  on each black-box model.** Each mountain-like curve shows the trade-off between diversity and stability of newborn models. All four curves reach the sweet spot at  $r = 0.7$ . (b): **The decay on the accuracy of each network with respect to the rate of parameters pruned.** With the prunable rate  $r = 0.7$ , there are 35% of weights pruned away in expectation at each iteration. The quantity is not harmful to the accuracy of the networks according to the curves.

## 5 Conclusion

In this paper, we propose Diversified Weight Pruning (DWP) leveraging network compression to improve the targeted transferability of adversarial attacks. DWP aims to produce more white-box models from the existing ones via network pruning for ensemble. Due to the over-parameterized property of neural networks, the performance of models newly produced by DWP is well-preserved. Experiments show that assuring the quality of networks participating in ensemble significantly influences targeted transferability. By evaluating DWP on ImageNet, we show that DWP improves the state-of-the-art simple transferable attacks, especially for challenging scenarios such as adversarially trained models

and distinct architectures. With the longitudinal ensemble, DWP benefits most of the existing attacks without imposing extra costs. We hope that our work can serve as a bridge between network compression and transferable attack, inspiring more collaboration.

## References

- Carlini, N.; and Wagner, D. A. 2017. Towards Evaluating the Robustness of Neural Networks. In *2017 IEEE Symposium on Security and Privacy, SP 2017, San Jose, CA, USA, May 22-26, 2017*, 39–57. IEEE Computer Society.
- Denil, M.; Shakibi, B.; Dinh, L.; Ranzato, M.; and de Freitas, N. 2013. Predicting Parameters in Deep Learning. In Burges, C. J. C.; Bottou, L.; Ghahramani, Z.; and Weinberger, K. Q., eds., *Advances in Neural Information Processing Systems 26: 27th Annual Conference on Neural Information Processing Systems 2013. Proceedings of a meeting held December 5-8, 2013, Lake Tahoe, Nevada, United States*, 2148–2156.
- Dong, Y.; Liao, F.; Pang, T.; Su, H.; Zhu, J.; Hu, X.; and Li, J. 2018. Boosting Adversarial Attacks With Momentum. In *2018 IEEE Conference on Computer Vision and Pattern Recognition, CVPR 2018, Salt Lake City, UT, USA, June 18-22, 2018*, 9185–9193. Computer Vision Foundation / IEEE Computer Society.
- Dong, Y.; Pang, T.; Su, H.; and Zhu, J. 2019. Evading Defenses to Transferable Adversarial Examples by Translation-Invariant Attacks. In *IEEE Conference on Computer Vision and Pattern Recognition, CVPR 2019, Long Beach, CA, USA, June 16-20, 2019*, 4312–4321. Computer Vision Foundation / IEEE.
- Duan, Y.; Zou, J.; Zhou, X.; Zhang, W.; Zhang, J.; and Pan, Z. 2022. Adversarial Attack via Dual-Stage Network Erosion.
- Frankle, J.; and Carbin, M. 2019. The Lottery Ticket Hypothesis: Finding Sparse, Trainable Neural Networks. In *7th International Conference on Learning Representations*,



- ICLR 2019, New Orleans, LA, USA, May 6-9, 2019. OpenReview.net.
- Gonzalez, R. C. 2009. *Digital image processing*. Pearson education india.
- Goodfellow, I.; Shlens, J.; and Szegedy, C. 2015. Explaining and Harnessing Adversarial Examples. In *International Conference on Learning Representations*.
- Han, S.; Pool, J.; Tran, J.; and Dally, W. J. 2015. Learning both Weights and Connections for Efficient Neural Network. In Cortes, C.; Lawrence, N. D.; Lee, D. D.; Sugiyama, M.; and Garnett, R., eds., *Advances in Neural Information Processing Systems 28: Annual Conference on Neural Information Processing Systems 2015, December 7-12, 2015, Montreal, Quebec, Canada*, 1135–1143.
- He, K.; Zhang, X.; Ren, S.; and Sun, J. 2016. Deep Residual Learning for Image Recognition. In *2016 IEEE Conference on Computer Vision and Pattern Recognition, CVPR 2016, Las Vegas, NV, USA, June 27-30, 2016*, 770–778. IEEE Computer Society.
- Huang, G.; Liu, Z.; van der Maaten, L.; and Weinberger, K. Q. 2017. Densely Connected Convolutional Networks. In *2017 IEEE Conference on Computer Vision and Pattern Recognition, CVPR 2017, Honolulu, HI, USA, July 21-26, 2017*, 2261–2269. IEEE Computer Society.
- Kurakin, A.; Goodfellow, I.; Bengio, S.; Dong, Y.; Liao, F.; Liang, M.; Pang, T.; Zhu, J.; Hu, X.; Xie, C.; Wang, J.; Zhang, Z.; Ren, Z.; Yuille, A.; Huang, S.; Zhao, Y.; Zhao, Y.; Han, Z.; Long, J.; Berdibekov, Y.; Akiba, T.; Tokui, S.; and Abe, M. 2018. Adversarial Attacks and Defences Competition.
- Kurakin, A.; Goodfellow, I. J.; and Bengio, S. 2017. Adversarial examples in the physical world. In *5th International Conference on Learning Representations, ICLR 2017, Toulon, France, April 24-26, 2017, Workshop Track Proceedings*. OpenReview.net.
- LeCun, Y.; Denker, J. S.; and Solla, S. A. 1989. Optimal Brain Damage. In Touretzky, D. S., ed., *Advances in Neural Information Processing Systems 2, [NIPS Conference, Denver, Colorado, USA, November 27-30, 1989]*, 598–605. Morgan Kaufmann.
- Li, C.; Gao, S.; Deng, C.; Xie, D.; and Liu, W. 2019. Cross-Modal Learning with Adversarial Samples. In Wallach, H. M.; Larochelle, H.; Beygelzimer, A.; d’Alché-Buc, F.; Fox, E. B.; and Garnett, R., eds., *Advances in Neural Information Processing Systems 32: Annual Conference on Neural Information Processing Systems 2019, NeurIPS 2019, December 8-14, 2019, Vancouver, BC, Canada*, 10791–10801.
- Li, M.; Deng, C.; Li, T.; Yan, J.; Gao, X.; and Huang, H. 2020a. Towards Transferable Targeted Attack. In *2020 IEEE/CVF Conference on Computer Vision and Pattern Recognition, CVPR 2020, Seattle, WA, USA, June 13-19, 2020*, 638–646. Computer Vision Foundation / IEEE.
- Li, Y.; Bai, S.; Zhou, Y.; Xie, C.; Zhang, Z.; and Yuille, A. L. 2020b. Learning Transferable Adversarial Examples via Ghost Networks. In *The Thirty-Fourth AAAI Conference on Artificial Intelligence, AAAI 2020, The Thirty-Second Innovative Applications of Artificial Intelligence Conference, IAAI 2020, The Tenth AAAI Symposium on Educational Advances in Artificial Intelligence, EAAI 2020, New York, NY, USA, February 7-12, 2020*, 11458–11465. AAAI Press.
- Lin, J.; Song, C.; He, K.; Wang, L.; and Hopcroft, J. E. 2020. Nesterov Accelerated Gradient and Scale Invariance for Adversarial Attacks. In *8th International Conference on Learning Representations, ICLR 2020, Addis Ababa, Ethiopia, April 26-30, 2020*. OpenReview.net.
- Liu, Y.; Chen, X.; Liu, C.; and Song, D. 2017. Delving into Transferable Adversarial Examples and Black-box Attacks. In *International Conference on Learning Representations*.
- Liu, Z.; Sun, M.; Zhou, T.; Huang, G.; and Darrell, T. 2019. Rethinking the Value of Network Pruning. In *7th International Conference on Learning Representations, ICLR 2019, New Orleans, LA, USA, May 6-9, 2019*. OpenReview.net.
- Madry, A.; Makelov, A.; Schmidt, L.; Tsipras, D.; and Vladu, A. 2018. Towards Deep Learning Models Resistant to Adversarial Attacks. In *6th International Conference on Learning Representations, ICLR 2018, Vancouver, BC, Canada, April 30 - May 3, 2018, Conference Track Proceedings*. OpenReview.net.
- NESTEROV, Y. 1983. A method for unconstrained convex minimization problem with the rate of convergence  $O(1/k^2)$ . In *Doklady AN USSR*, volume 269, 543–547.
- Shorten, C.; and Khoshgoftaar, T. M. 2019. A survey on Image Data Augmentation for Deep Learning. *J. Big Data*, 6: 60.
- Simonyan, K.; and Zisserman, A. 2015. Very Deep Convolutional Networks for Large-Scale Image Recognition. In Bengio, Y.; and LeCun, Y., eds., *3rd International Conference on Learning Representations, ICLR 2015, San Diego, CA, USA, May 7-9, 2015, Conference Track Proceedings*.
- Srivastava, N.; Hinton, G. E.; Krizhevsky, A.; Sutskever, I.; and Salakhutdinov, R. 2014. Dropout: a simple way to prevent neural networks from overfitting. *J. Mach. Learn. Res.*, 15(1): 1929–1958.
- Szegedy, C.; Ioffe, S.; Vanhoucke, V.; and Alemi, A. A. 2017. Inception-v4, Inception-ResNet and the Impact of Residual Connections on Learning. In Singh, S.; and Markovitch, S., eds., *Proceedings of the Thirty-First AAAI Conference on Artificial Intelligence, February 4-9, 2017, San Francisco, California, USA*, 4278–4284. AAAI Press.
- Szegedy, C.; Vanhoucke, V.; Ioffe, S.; Shlens, J.; and Wojna, Z. 2016. Rethinking the Inception Architecture for Computer Vision. In *2016 IEEE Conference on Computer Vision and Pattern Recognition, CVPR 2016, Las Vegas, NV, USA, June 27-30, 2016*, 2818–2826. IEEE Computer Society.
- Szegedy, C.; Zaremba, W.; Sutskever, I.; Bruna, J.; Erhan, D.; Goodfellow, I.; and Fergus, R. 2014. Intriguing properties of neural networks. In *International Conference on Learning Representations*.
- Tramèr, F.; Kurakin, A.; Papernot, N.; Goodfellow, I. J.; Boneh, D.; and McDaniel, P. D. 2018. Ensemble Adversarial Training: Attacks and Defenses. In *6th International*

*Conference on Learning Representations, ICLR 2018, Vancouver, BC, Canada, April 30 - May 3, 2018, Conference Track Proceedings*. OpenReview.net.

Wang, X.; He, X.; Wang, J.; and He, K. 2021. Admix: Enhancing the Transferability of Adversarial Attacks. In *2021 IEEE/CVF International Conference on Computer Vision, ICCV 2021, Montreal, QC, Canada, October 10-17, 2021*, 16138–16147. IEEE.

Xie, C.; Zhang, Z.; Zhou, Y.; Bai, S.; Wang, J.; Ren, Z.; and Yuille, A. L. 2019. Improving Transferability of Adversarial Examples With Input Diversity. In *IEEE Conference on Computer Vision and Pattern Recognition, CVPR 2019, Long Beach, CA, USA, June 16-20, 2019*, 2730–2739. Computer Vision Foundation / IEEE.

Xiong, Y.; Lin, J.; Zhang, M.; Hopcroft, J. E.; and He, K. 2022. Stochastic Variance Reduced Ensemble Adversarial Attack for Boosting the Adversarial Transferability. In *Proceedings of the IEEE/CVF Conference on Computer Vision and Pattern Recognition (CVPR)*, 14983–14992.

Yuan, H.; Chu, Q.; Zhu, F.; Zhao, R.; Liu, B.; and Yu, N.-H. 2021. AutoMA: Towards Automatic Model Augmentation for Transferable Adversarial Attacks. *IEEE Transactions on Multimedia*, 1–1.

Zhang, H.; Cissé, M.; Dauphin, Y. N.; and Lopez-Paz, D. 2018. mixup: Beyond Empirical Risk Minimization. In *6th International Conference on Learning Representations, ICLR 2018, Vancouver, BC, Canada, April 30 - May 3, 2018, Conference Track Proceedings*. OpenReview.net.

Zhao, Z.; Liu, Z.; and Larson, M. 2021. On Success and Simplicity: A Second Look at Transferable Targeted Attacks. In Ranzato, M.; Beygelzimer, A.; Dauphin, Y.; Liang, P.; and Vaughan, J. W., eds., *Advances in Neural Information Processing Systems*, volume 34, 6115–6128. Curran Associates, Inc.

Zou, J.; Duan, Y.; Li, B.; Zhang, W.; Pan, Y.; and Pan, Z. 2022. Making Adversarial Examples More Transferable and Indistinguishable. In *Thirty-Sixth AAAI Conference on Artificial Intelligence, AAAI 2022, Thirty-Fourth Conference on Innovative Applications of Artificial Intelligence, IAAI 2022, The Twelveth Symposium on Educational Advances in Artificial Intelligence, EAAI 2022 Virtual Event, February 22 - March 1, 2022*, 3662–3670. AAAI Press.